Inorg. Chem. **2006**, *45*, 3538–3548

Syntheses, Crystal Structures, and Magnetic Characterization of Five New Dimeric Manganese(III) Tetradentate Schiff Base Complexes Exhibiting Single-Molecule-Magnet Behavior

Zhengliang Lu,[†,§,#] Mei Yuan,[‡,#] Feng Pan,[‡] Song Gao,*[,‡] Deqing Zhang,*[,†] and Daoben Zhu[†]

Beijing National Laboratory for Molecular Sciences, Organic Solids Laboratory, Institute of Chemistry, Chinese Academy of Sciences, Beijing 100080, China, State Key Laboratory of Rare Earth Materials Chemistry and Applications, College of Chemistry and Molecular Engineering, Peking University, Beijing 100875, China, and Graduate School of Chinese Academy of Sciences, Beijing 100080, China

Received September 25, 2005

Tetradentate Schiff base ligands H_2L (H_2saltmen, H_2salen, H_2-5-Brsalen, and H_2-3,5-Brsalen), derived from the condensation of the corresponding salicylaldehyde or its derivatives with 1,1,2,2-tetramethylethyldiamine or 1, 2-diaminoethane, reacted with Mn^{III} acetate or perchlorate salts and sodium azide or sodium cyanate to produce five Mn^{III} dimer complexes, $[Mn(saltmen)(O_2CCH_3)]_2 \cdot 2CH_3CO_2H$ (**1**), $[Mn(saltmen)(N_3)]_2$ (**2**), $[Mn(salen)(NCO)]_2$ (**3**), $[Mn(3,5\text{-Brsalen})(3,5\text{-Brsalicylaldehyde})]_2$ (**4**), and $[Mn(5\text{-Brsalen})(CH_3OH)]_2(ClO_4)_2$ (**5**). These new complexes have been characterized by IR, elemental analyses, crystal structural analyses, and magnetic studies. Within these Mn^{III} dimeric complexes, two Mn^{III} ions are connected by phenolate oxygen atoms with acetate, azide, cyanate, a 3,5-Brsalicyladehyde anion, and a neutral methanol molecule as the axial ligands for complexes **1**–**5**, respectively. Complexes **1**–**4** exhibit intradimer ferromagnetic exchange and display frequency dependence of *ac* magnetic susceptibility, possibly showing single-molecule-magnet (SMM) behavior. In contrast, complex **5** shows an intradimer antiferromagnetic coupling probably originating from the relatively shorter Mn–O* distance, compared to those of complexes **1**–**4**.

Introduction

In recent years, the research on single-molecule magnets (SMMs)[1−5] and single-chain magnets (SCMs)[6−10] has received significant attention in the area of molecular magnetism. SMMs exhibit slow relaxation of their magnetization induced by the combined effect of a high-spin ground state S_T and uniaxial anisotropy D, which generate an energy barrier between spin-up and spin-down states. Thus, SMMs are potentially useful for information storage at the molecular

* To whom correspondence should be addressed. E-mail: gaosong@pku.edu.cn (S.G.); dqzhang@iccas.ac.cn (D.-Q.Z.).
† Institute of Chemistry, Chinese Academy of Sciences.
‡ College of Chemistry and Molecular Engineering, Peking University.
§ Graduate School of Chinese Academy of Sciences.
# Mr. Lü and Ms. Yuan contributed equally to the present work.

(1) For examples, see: (a) Christou, G.; Gatteschi, D.; Hendrickson, D. N.; Sessoli, R. *MRS Bull.* **2000**, *25*, 66. (b) Gatteschi, D.; Sessoli, R. *Angew. Chem., Int. Ed.* **2003**, *42*, 268. (c) Boyd, P. D. W.; Li, Q.; Vincent, J. B.; Folting, K.; Chang, H.; Streib, W. E.; Huffman, J. C.; Christou, G.; Hendrickson, D. N. *J. Am. Chem. Soc.* **1988**, *110*, 8537. (d) Sessoli, R.; Tsai, H.; Schake, A. R.; Wang, S.; Vincent, J. B.; Folting, D.; Gatteschi, D.; Christou, G.; Hendrickson, D. N. *J. Am. Chem. Soc.* **1993**, *115*, 1804. (e) Yoo, J.; Brechin, E. K.; Yamaguchi, A.; Nakano, M.; Huffman, J. C.; Maniero, A. L.; Brunel, L.; Awaga, K.; Ishimoto, H.; Christou, G.; Hendrickson, D. N. *Inorg. Chem.* **2000**, *39*, 3615. (f) Boskovic, C.; Brechin, E. K.; Streib, W. E.; Folting, K.; Hendrickson, D. N.; Christou, G. *J. Am. Chem. Soc.* **2002**, *124*, 3725. (g) Castro, S. L.; Sun, Z.; Grant, C. M.; Bollinger, J. C.; Hendrickson, D. N.; Christou, G. *J. Am. Chem. Soc.* **1998**, *120*, 2365.
(2) Caneschi, A.; Gatteschi, D.; Sessoli, R. *J. Am. Chem. Soc.* **1991**, *113*, 5837.
(3) Barra, A. L.; Caneschi, A.; Cornia, A.; Fabrizi, F.; de Biani, D.; Gatteschi, D.; Sangregorio, C.; Sessoli, R.; Sorace, L. *J. Am. Chem. Soc.* **1999**, *121*, 5302.
(4) Cadiou, C.; Murrie, M.; Paulsen, C.; Villar, V.; Wernsdorfer, W.; Winpenny, R. E. P. *Chem. Commun.* **2001**, 2666.
(5) Sokol, J. J.; Hee, A. G.; Long, J. R. *J. Am. Chem. Soc.* **2002**, *124*, 7656.
(6) Caneschi, A.; Gatteschi, D.; Lalioti, N.; Sangregorio, C.; Sessoli, R.; Venturi, G.; Vindigni, A.; Rettori, A.; Pini, M. G.; Novak, M. *Angew. Chem., Int. Ed.* **2001**, *40*, 1760.
(7) Clérac, R.; Miyasaka, H.; Yamashita, M.; Coulon, C. *J. Am. Chem. Soc.* **2002**, *124*, 12837.
(8) Miyasaka, H.; Clérac, R.; Mizushima, K.; Sugiura, K.; Yamashita, M.; Wernsdorfer, W.; Coulon, C. *Inorg. Chem.* **2003**, *42*, 8203.
(9) Lescouëzec, R.; Vaissermann, J.; Ruiz-Pérez, C.; Lloret, F.; Carrasco, M.; Julve, M.; Verdaguer, M.; Dromzée, Y.; Gatteschi, D.; Wernsdorfer, W. *Angew. Chem., Int. Ed.* **2003**, *42*, 1483.
(10) (a) Liu, T.; Fu, D.; Gao, S.; Zhanu, Y.; Sun, H.; Su, G.; Liu, Y. *J. Am. Chem. Soc.* **2003**, *125*, 13976. (b) Pardo, E.; Ruiz-García, R.; Lloret, F.; Faus, J.; Julve, M.; Journaux, Y.; Delgado, F.; Ruiz-Pérez, C. *Adv. Mater.* **2004**, *16*, 1597.

10.1021/ic051648l CCC: $33.50
Published on Web 04/07/2006

level. Moreover, SMMs are considered to be unique systems for studying quantum spin tunneling and quantum phase interference, which may lead to the application of SMMs in molecular electronics.[11]

Among the reported SMMs, the Mn^{III} complexes play very important roles. For instance, the first SMM is a Mn_{12} complex.[12] In addition to the Mn_{12} complexes, several Mn_4 complexes were found to be SMMs.[13−18] Miyasaka et al.[19] further minimized the nuclearity of SMMs based on Mn^{III} complexes and reported a dimeric manganese(III) tetradenate Schiff base complex showing SMM behavior. In fact, tens of dimeric Mn^{III} complexes were described previously,[20−30]

Scheme 1

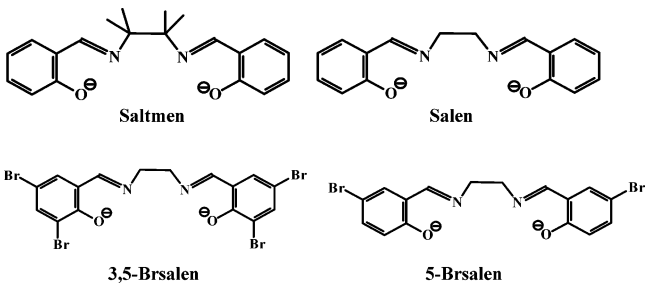

and some of them were magnetically characterized. Both ferromagnetic and antiferromagnetic interactions between the two Mn^{III} ions were reported. Modulation of the $Mn^{III}\cdots Mn^{III}$ magnetic interaction by varying the apical ligands and the chemical features of the Schiff base ligand through changing the corresponding diamines seems to be possible when the structures of the dimeric Mn^{III} complexes are considered. Herein we report five new dimeric manganese(III) tetradenate schiff base complexes: $[Mn(saltmen)(O_2CCH_3)]_2\cdot 2CH_3CO_2H$ (**1**), $[Mn(saltmen)(N_3)]_2$ (**2**), $[Mn(salen)(NCO)]_2$ (**3**), [Mn-(3,5-Brsalen)(3,5-Brsalicyladehyde)]$_2$ (**4**), and $[Mn(5\text{-Brsalen})(CH_3OH)]_2(ClO_4)_2$ (**5**). The corresponding Schiff base ligands used in this paper were listed in Scheme 1. Within these new dimeric Mn^{III} complexes, two Mn^{III} ions are connected by phenolate oxygen atoms with acetate, azide, cyanate, a 3,5-Brsalicyladehyde anion, and a neutral methanol molecule as the axial ligands for complex **1**−**5**, respectively. Magnetic studies indicate that complexes **1**−**4** exhibit obvious ferromagnetic coupling between the two Mn^{III} ions and frequency dependence of *ac* magnetic susceptibility, one of the most important characteristic behaviors of SMMs, while the two Mn^{III} ions are antiferromagnetically coupled in complex **5**.

Experimental Section

Materials and Measurements. All the chemicals used in syntheses were of reagent grade and were used without further purification. The tetradentate Schiff base ligands H_2L (H_2saltmen, H_2salen, H_2-5-Brsalen, and H_2-3,5-Brsalen) were synthesized by mixing the corresponding salicylaldehyde or its derivatives and 1,1,2,2-tetramethylethyldiamine or 1, 2-diaminoethane in a 2:1 mole ratio in ethanol.

Caution: Although we have experienced no problem with complexes **2**−**5** reported in this work, perchlorate salts and sodium azide are potentially explosive and should be handled in small quantities and very carefully.

Infrared spectra were recorded as KBr pellets on a Perkin-Elmer Paragon 1000 FT-IR spectrometer. Elemental analyses were carried out on a Perkin-Elmer 240C analyzer. Magnetic measurements were carried out on an Oxford Maglab 2000 System or a Quantum Design

(11) (a) Wernsdorfer, W.; Sessoli, R. *Science* **1999**, *284*, 133. (b) Leuenberger, M. N.; Loss, D. *Nature* **2001**, *410*, 789.
(12) (a) Boyd, P. D. W.; Li, Q.; Vincent, J. B.; Folting, K.; Chang, H.; Streib, W. E.; Huffman, J. C.; Christou, G.; Hendrickson, D. N. *J. Am. Chem. Soc.* **1988**, *110*, 8537. (b) Caneschi, A.; Gatteschi, D.; Sessoli, R.; Barra, A. L.; Brunel, L. C.; Guillot, M. *J. Am. Chem. Soc.* **1991**, *113*, 5873. (c) Sessoli, R.; Tsai, H.; Schake, A. R.; Wang, S.; Vincent, J. B.; Folting, K.; Gatteschi, D.; Christou, G.; Hendrickson, D. N. *J. Am. Chem. Soc.* **1993**, *115*, 1804. (d) Sessoli, R.; Gatteschi, D.; Caneschi, A.; Novak, A. M. *Nature* **1993**, *365*, 141. (e) Aubin, S. M. J.; Wemple, M. W.; Adams, D. M.; Tsai, H. L.; Christou, G.; Hendrickson, D. N. *J. Am. Chem. Soc.* **1996**, *118*, 7746. (f) Aubin, S. M. J.; Dilley, N. R.; Pardi, L.; Krzystek, J.; Wemple, M. W.; Brunel, L. C.; Maple, M. B.; Christou, G.; Hendrickson, D. N. *J. Am. Chem. Soc.* **1998**, *120*, 4991. (g) Aubin, S. M. J.; Spagna, S.; Eppley, H. J.; Sager, R. E.; Christou, G.; Hendrickson, D. N. *Chem. Commun.* **1998**, 803.
(13) (a) Boskovic, C.; Bircher, R.; Tregenna-Piggott, P. L. W.; Güdel, H. U.; Paulsen, C.; Wernsdorfer, W.; Barra, A.-L.; Khatsko, E.; Neels, A.; Stoecki-Evans, H. *J. Am. Chem. Soc.* **2003**, *125*, 14046. (b) Lecren, L.; Wernsdorfer, W.; Li, Y.; Roubeau, O.; Miyasaka, H.; Clérac, R. *J. Am. Chem. Soc.* **2005**, *127*, 11311. (c) Wittick, L. M.; Murray, K. S.; Moubaraki, B.; Batten, S. R.; Spiccia, L.; Berry, K. J. *Dalton Trans.* **2004**, 1003. (d) Lecren, L.; Li, Y.; Wernsdorfer, W.; Roubeau, O.; Miyasaka, H.; Clérac, R. *Inorg. Chem. Commun.* **2005**, *8*, 626.
(14) Libby, E.; McCusker, J. K.; Schmitt, E. A.; Folting, K.; Hendrickson, D. N.; Christou, G. *Inorg. Chem.* **1991**, *30*, 3486.
(15) (a) Yoo, J.; Brechin, E. K.; Yamaguchi, A.; Nakano, M.; Huffman, J. C.; Maniero, A. L.; Brunel, L.; Awaga, K.; Ishimoto, H.; Christou, G.; Hendrichson, D. N. *Inorg. Chem.* **2000**, *39*, 3615. (b) Yoo, J.; Yamaguchi, A.; Nakano, M.; Krzystek, J.; Streib, W. E.; Brunel, L.; Ishimoto, H.; Christou, G.; Hendrickson, D. N. *Inorg. Chem.* **2001**, *40*, 4604.
(16) (a) Aliaga-Alcalde, N.; Edwards, R. S.; Hill, S. O.; Wernsdorfer, W.; Folting, K.; Christou, G. *J. Am. Chem. Soc.* **2004**, *126*, 12503. (b) Aromí, G.; Bhaduri, S.; Artús, P.; Folting, K.; Christou, G. *Inorg. Chem.* **2002**, *41*, 805. (c) Andres, H.; Basler, R.; Güdel, H.-U.; Aromí, G.; Christou, G.; Büttner, H.; Rufflé, B. *J. Am. Chem. Soc.* **2000**, *122*, 12469. (d) Aliaga, N.; Folting, K.; Hendrickson, D. N.; Christou, G. *Polyhedron* **2001**, *20*, 1273. (e) Cañada-Vilalta, C.; Huffman, J. C.; Christou, G. *Polyhedron* **2001**, *20*, 1785. (f) Wang, S.; Wemple, M. S.; Yoo, J.; Folting, K.; Huffman, J. C.; Hagen, K. S.; Hendrickson, D. N.; Christou, G. *Inorg. Chem.* **2000**, *39*, 1501.
(17) Yang, E.; Harden, N.; Wernsdorfer, W.; Zakharov, L.; Brechin, E. K.; Rheingold, A. L.; Christou, G.; Hendrickson, D. N. *Polyhedron* **2003**, *22*, 1857.
(18) Brechin, E. K.; Yoo, J.; Nakano, M.; Huffman, J. C.; Hendrickson, D. N.; Christou, G. *Chem. Commun.* **1999**, 783.
(19) Miyasaka, H.; Clérac, R.; Wernsdorfer, W.; Lecren, L.; Bonhomme, C.; Sugiura, K.; Yamashita, M. *Angew. Chem., Int. Ed.* **2004**, *43*, 2801.
(20) Karmakar, R.; Choudhury, C. R.; Bravic, G.; Sutter, J.-P.; Mitra. S. *Polyhedron* **2004**, *23*, 949.
(21) Shyu, H.; Wei, H.; Wang, Y. *Inorg. Chim. Acta* **1999**, *290*, 8.
(22) (a) Mabad, B.; Luneau, D.; Theil, S.; Dahan, F.; Savariault, J. M.; Tuchagues, J. P. *J. Inorg. Biochem.* **1991**, *43*, 373. (b) Kennedy, B. J.; Murray, K. S. *Inorg. Chem.* **1985**, *24*, 1552.
(23) Miyasaka, H.; Clérac, R.; Ishii, T.; Chang, H.; Kitagawa, S.; Yamashita, M. *J. Chem. Soc., Dalton Trans.* **2002**, 1528.
(24) Bermejo, M. R.; Castiñeiras, A.; Garcia-Montergudo, J. C.; Rey, M.; Sousa, A.; Watkinson, M.; McAuliffe, C. A.; Pritchard, R. G.; Beddoes. R. L. *J. Chem. Soc., Dalton Trans.* **1996**, 2935.
(25) Matsumoto, N.; Zhong, Z.;Ōkawa, H.; Kida, S. *Inorg. Chim. Acta* **1989**, *160*, 153.
(26) (a) Matsumoto, N.; Takemoto, N.; Ohyosi, A.; Ōkawa, H. *Bull. Chem. Soc. Jpn.* **1988**, *61*, 2984. (b) Mikuriya, M.; Yamato, Y.; Tokii, T. *Bull. Chem. Soc. Jpn.* **1992**, *65*, 1466.
(27) Garcia-Deibe, A.; Sousa, A.; Bermejo, M. R.; MacRory, P. P.; McAuliffe, C. A.; Pritchard, R. G.; Helliwell, M. *J. Chem. Soc., Chem. Commun.* **1991**, 728.
(28) Miyasaka, H.; Sugimoto, K.; Sugiura, K.; Ishii, T.; Yamashita, M. *Mol. Cryst. Liq. Cryst.* **2002**, *379*, 197.
(29) Miyasaka, H.; Mizushima, K.; Furukawa, S.; Sugiura, K.; Ishii, T.; Yamashita, M. *Mol. Cryst. Liq. Cryst.* **2002**, *379*, 171.
(30) Sato, Y.; Miyasaka, H.; Matsumoto, N.; Ōkawa, H. *Inorg. Chim. Acta* **1996**, *247*, 57.

Table 1. Crystallographic and Refinement Data for Complexes **1**−**5**

	1	**2**	**3**	**4**	**5**
formula	$C_{48}H_{58}Mn_2N_4O_{12}$	$C_{40}H_{44}Mn_2N_{10}O_4$	$C_{34}H_{28}Mn_2N_6O_6$	$C_{46}H_{26}Br_{12}Mn_2N_4O_8$	$C_{34}H_{32}Br_4Cl2Mn_2N_4O_{14}$
fw	992.86	838.74	726.50	1831.51	1221.06
cryst syst	monoclinic	monoclinic	orthorhombic	monoclinic	monoclinic
space group	$P2_1/c$	$P2_1/c$	*Pbca*	$P2_1/c$	$P2_1/n$
a (Å)	11.024(2)	8.0512(16)	13.131(3)	12.606(3)	11.019(2)
b (Å)	18.905(4)	16.874(3)	14.177(3)	15.713(3)	13.047(3)
c (Å)	12.107(2)	14.346(3)	16.710(3)	14.343(3)	14.914(3)
α (deg)	90	90	90	90	90
β (deg)	105.42(3)	103.84(3)	90	115.67(3)	102.78(3)
γ (deg)	90	90	90	90	90
V (Å^3)	2432.4(8)	1892.5(7)	3110.7(11)	2560.6(9)	2090.9(7)
Z	2	2	4	2	2
ρ_{calcd} (Mg/m^3)	1.356	1.472	1.551	2.375	1.939
μ (mm^{-1})	0.583	0.724	0.869	9.914	4.624
F(000)	1040	872	1488	1728	1200
reflns collected	23 257	5737	44 409	41 120	37 369
unique reflns	9072	3753	3548	4752	34 800
GOF	1.080	0.870	0.951	1.073	0.995
final R indices	R1[a]=0.0604	R1=0.0812	R1=0.0346	R1=0.0703	R1=0.0495
[$I > 2\sigma(I)$]	wR2[b]=0.1425	wR2=0.1488	wR2=0.0603	wR2=0.2118	wR2=0.1195
R indices	R1 = 0.0792	R1=0.1923	R1=0.1110	R1=0.1178	R1=0.0909
(all data)	wR2 = 0.1537	wR2=0.1867	wR2=0.0696	wR2=0.2315	wR2=0.1333

[a] $R1 = \Sigma||F_o| - |F_c||/\Sigma|F_o|$. [b] $wR2 = \sum[w(F_o^2 - F_c^2)^2]/\sum[w(F_o^2)^2]^{1/2}$.

MPMS-XL5 SQUID magnetometer. The diamagnetic corrections were calculated from Pascal's constants.

X-ray Crystallographic Study. Single-crystal X-ray diffraction data for complexes **1** and **2** were collected on a Rigaku R-AXIS RAPID IP diffractometer at 293 K using graphite-monochromated Mo Kα radiation (λ = 0.71073 Å) and the oscillation scans technique in the range of $1.85° < \theta < 27.48°$, while those for compounds **3**−**5** were collected using a NONIUS Kappa-CCD diffractometer with Mo Kα radiation (λ = 0.71073 Å) at 293 K. The structures were solved by direct methods using the program SHELXS-97[31] and refined by full-matrix least-squares methods on F^2 using SHELXL-97.[32] All non-hydrogen atoms were refined anisotropically. Hydrogen atoms defined by the stereochemistry were placed at their calculated positions and allowed to ride on their host carbons in coordinates. A summary of the crystallographic data and structural determination and refinement details for complexes **1**−**5** is provided in Table 1.

Preparation of Complex 1. A solution of manganese(III) acetate dihydrate (0.27 g, 1.0 mmol) in methanol (10 mL) was added to H_2saltmen (0.32 g, 1.0 mmol) in methanol (20 mL). After the brown solution was heated to 50 °C and stirred for 30 min, 10 mL of water was added to the reaction mixture, and it was filtered. The red-black solution collected was left to stand for one week at room temperature to form dark brown crystals. The crystals were collected by suction filtration (yield of 81% based on manganese(III) acetate dihydrate). Anal. Calcd for $C_{48}H_{58}Mn_2N_4O_{12}$: C, 58.07; H, 5.89; N, 5.65. Found: C, 58.09; H, 5.83; N, 5.68. IR (KBr, cm^{-1}): 1723, 1605, 1543, 1469, 1442, 1398, 1290, 1146, 757, 626.

Preparation of Complex 2. A solution of $Mn(ClO_4)_2{\cdot}6H_2O$ (0.36 g, 1.0 mmol) in methanol (20 mL) was added to H_2saltmen (0.32 g, 1.0 mmol) in methanol (20 mL), followed by the addition of Et_3N (0.14 mL, 1.0 mmol). The solution was refluxed for 1 h before solid NaN_3 (0.07 g, 1.0 mmol) was added. Hot water (10 mL) was added to the hot solution in methanol. The filtrate was collected and left to stand for several weeks at room temperature. The dark brown crystals were collected by filtration (62% yield based on Mn). Anal. Calcd for $C_{40}H_{44}Mn_2N_{10}O_4$: C, 57.26; H, 5.29; N, 16.71. Found: C, 56.71; H, 5.22; N, 16.58. IR (KBr, cm^{-1}): 2040, 1604, 1540, 1466, 1441, 1393, 1299, 1144, 751, 626.

Preparation of Complex 3. A solution of $Mn(ClO_4)_2{\cdot}6H_2O$ (0.36 g, 1.0 mmol) in methanol (20 mL) was added to H_2salen (0.32 g, 1.0 mmol) in methanol (20 mL), followed by the addition of Et_3N (0.28 mL, 2.0 mmol). The solution was heated to 50 °C and stirred for 2 h; then NaOCN (0.07 g, 1.0 mmol) dissolved in a minimum of water was added. After another 2 h, the filtrate was collected and left to stand for several weeks at room temperature. The dark brown crystals were collected by filtration (90% yield based on Mn). Anal. Calcd for $C_{34}H_{28}Mn_2N_6O_6$: C, 56.21; H, 3.88; N, 11.57. Found: C, 56.05; H, 3.86; N, 11.43. IR (KBr, cm^{-1}): 3019, 2948, 2170, 2164, 1623, 1601, 1542, 1468, 1446, 1296, 904, 800, 760.

Preparation of Complex 4. A solution of $Mn(ClO_4)_2{\cdot}6H_2O$ (0.09 g, 0.25 mmol) in methanol (5 mL) was added to H_2-3, 5-Brsalen (0.11 g, 0.25 mmol) in methanol (20 mL), followed by the addition of solid NaOH (0.02 g, 0.50 mmol). The solution was refluxed for 4 h, and then the filtrate was collected and left to stand for several weeks at room temperature. The dark brown crystals were collected by filtration (45% yield based on Mn). Anal. Calcd for $C_{46}H_{26}Br_{12}Mn_2N_4O_8$: C, 30.17; H, 1.43; N, 3.06. Found: C, 30.25; H, 1.46; N, 2.92. IR (KBr, cm^{-1}): 3063, 2925, 2854, 1623, 1581, 1510, 1436, 1408, 1375, 1294, 1213, 1167, 747, 722.

Preparation of Complex 5. A solution of $Mn(ClO_4)_2{\cdot}6H_2O$ (0.09 g, 0.25 mmol) in methanol (5 mL) was added to H_2-5-Brsalen (0.09 g, 0.25 mmol) in methanol (20 mL), followed by the addition of NaOH (0.02 g, 0.50 mmol). The solution was heated to 50 °C and stirred for 2 h. The filtrate was collected and left to stand for several weeks at room temperature. The dark brown crystals were collected by filtration (62% yield based on Mn). Anal. Calcd for $C_{34}H_{32}Br_4Cl_2Mn_2N_4O_{14}$: C, 33.44; H, 2.64; N, 4.59. Found: C, 33.31; H, 2.58; N, 4.50. IR (KBr, cm^{-1}): 3600, 3491, 3319, 1627, 1612, 1528, 1456, 1371, 1286, 1263, 1112, 831, 809, 689, 655.

Results and Discussion

Syntheses. Compounds **1**−**5** were prepared as dark brown crystals by slow evaporation of the resulting methanol

(31) Sheldrick, G. M. *SHELXL97, Program for Crystal Structure Refinement*; University of Göttingen: Göttingen, Germany, 1998.
(32) Sheldrick, G. M. *SHELXS97, Program for Crystal Structure Solution*; University of Göttingen: Göttingen, Germany, 1998; *Acta Crystallogr.* **1990**, *A46*, 467.

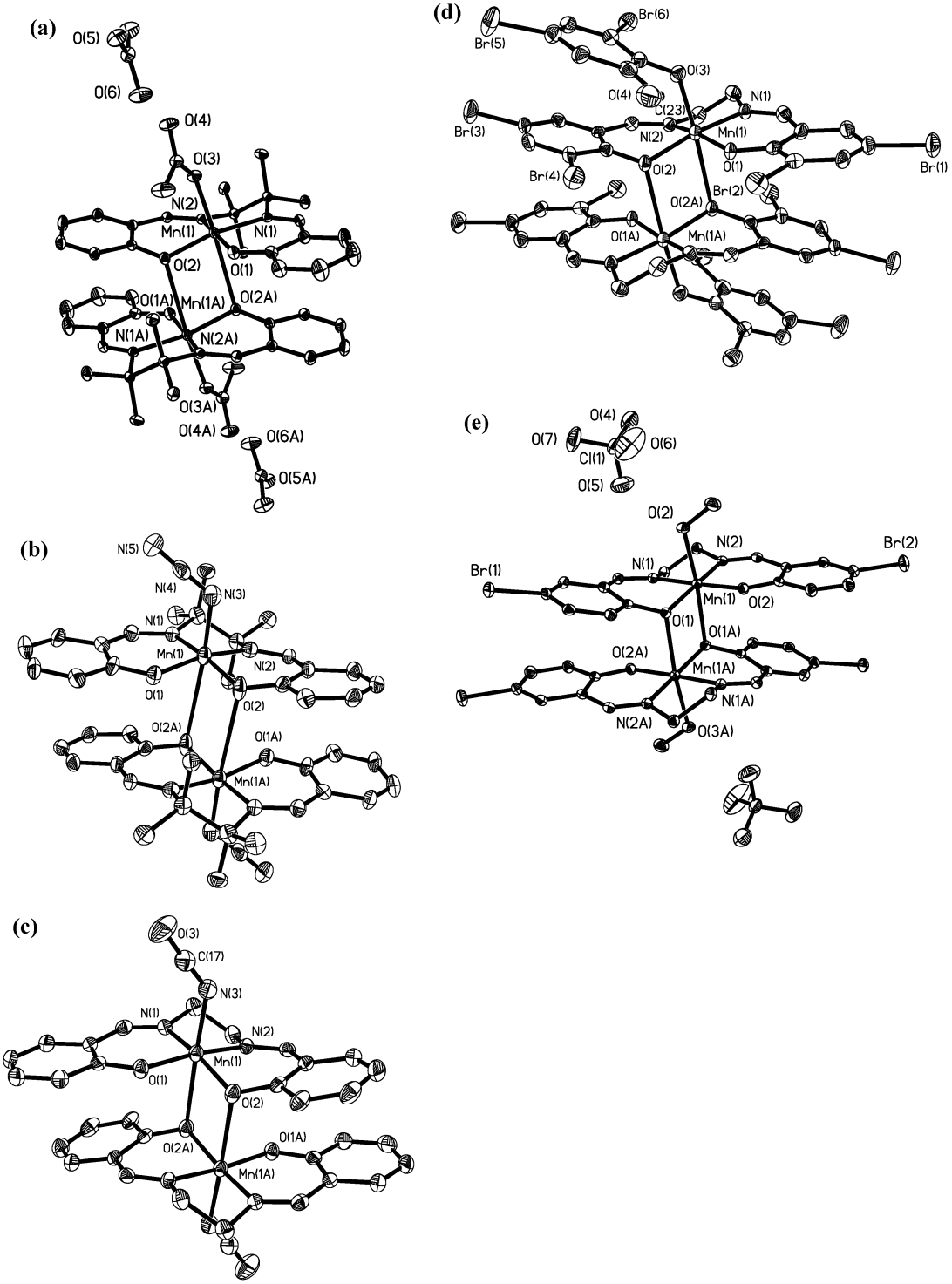

Figure 1. ORTEP drawings of the Mn^{III} dimers for complexes **1**−**5**: (a) **1**, (b) **2**, (c) **3**, (d) **4**, and (e) **5**.

solution with a small amount of water. During the preparation, heating and stirring were needed to favor the reactions. To get more examples for the investigation of the magnetic coupling rule of Mn^{III} dimer complexes, we chose four types of Schiff base ligands as secondary ligands including H_2-saltmen, H_2salen, H_2-5-Brsalen, and H_2-3,5-Brsalen, as well as five axial ligands for controlling the resulting compounds. Complex **1** was synthesized using a literature method with manganese(III) acetate dihydrate as the starting material, and the acetate group acts as the axial ligand in the resulting product. In complexes **2**−**5**, divalent $Mn(ClO_4)_2 \cdot 6H_2O$ was substituted for manganese(III) acetate dihydrate as the starting material to avoid the coordination of CH_3COO^-; in the reaction, the Mn^{II} ion may be oxidized by the oxygen in the atmosphere to Mn^{III} ion in the product in combination with the basic atmosphere. As a result, complexes **2**−**5** were obtained with azide, cyanate, a 3,5-Brsalicyladehyde anion, and a neutral methanol molecule as the axial ligands,

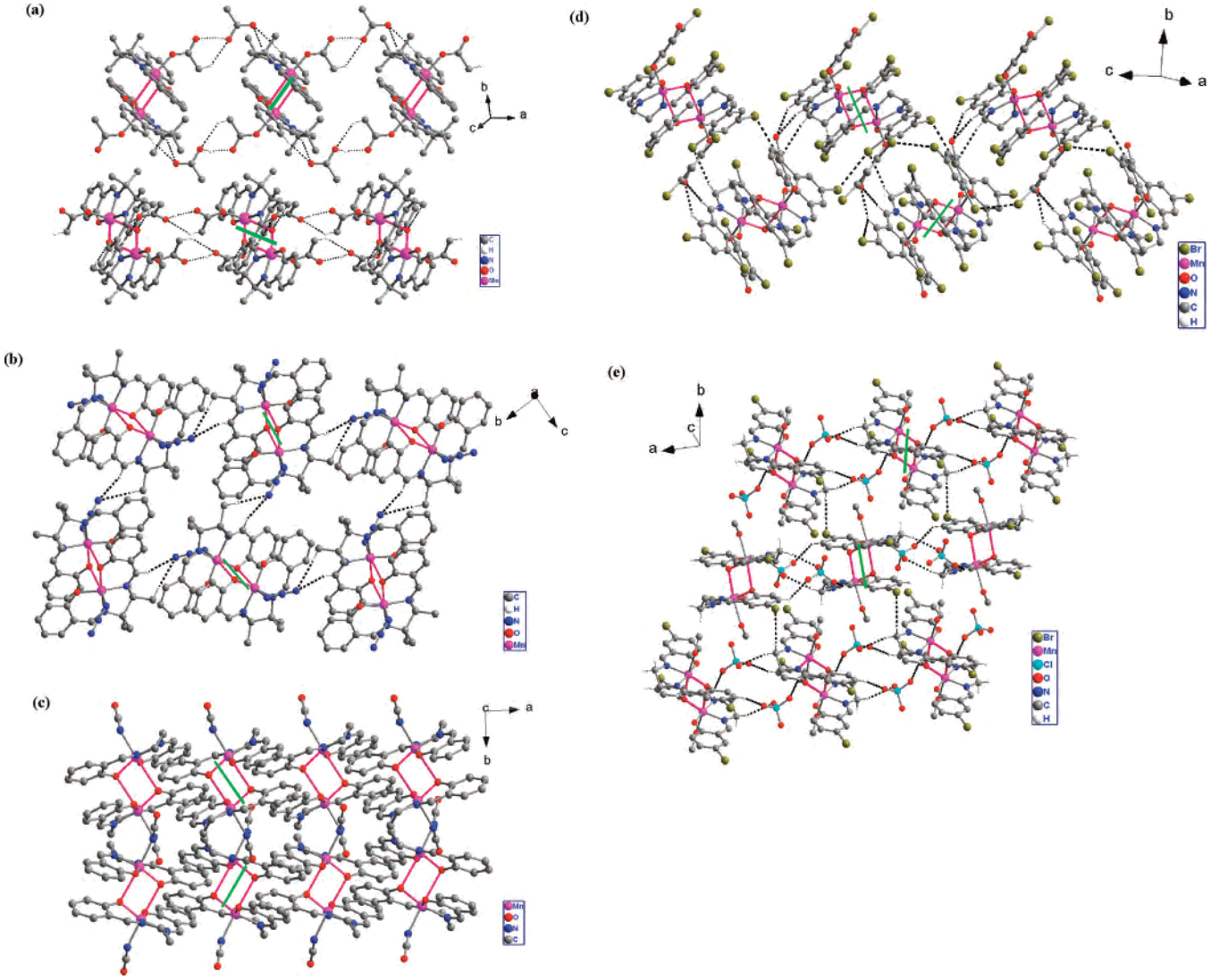

Figure 2. Crystal packing for complexes **1**−**5**. The green lines display the Jahn−Teller distortions of two symmetry-related Mn^{III} dimers: (a) **1**, (b) **2**, (c) **3**, (d) **4**, and (e) **5**.

respectively. The 3,5-Brsalicyladehyde anion originated from the decomposition of the 3,5-Brsalen ligand caused by refluxing in a strong basic environment.

FTIR Spectra. The IR spectra of compounds **1**−**5** exhibit strong absorption at 1600−1630 cm^{-1}, assignable to the ν(C═N or C═O) absorption. Also, the characteristic absorption of CH or NH groups is detected in a range of 2900−3350 cm^{-1}. For compounds **2**−**3**, the strong absorption at about 2000−2200 cm^{-1} is attributed to the asymmetric stretching vibration of azide or cyanate groups. The strong absorption peak for vibration of ClO_4^- is also observed at about 1100 cm^{-1} in compound **5**.

Crystal Structures. The structures of all five Mn^{III} complexes are similar to those of dimeric Mn^{III} complexes reported previously.[20−30] Each complex can be described as a dimer of [Mn(L)(X)], where L and X are the tetradentate Schiff base ligand (L = saltmen^{2-}, salen^{2-}, 5-Brsalen^{2-}, and 3,5-Brsalen^{2-}) and the corresponding axial ligand (X = CH_3COO^-, N_3^-, NCO^-, 3,5-Brsalicyladehyde anion, and CH_3OH), respectively. Two units of [Mn(L)(X)] are connected through Mn^{III}−O* bonding, where the O* atom refers to the phenolate oxygen atom of the another [Mn(L)(X)] unit. For complexes **1**−**5**, the local coordination geometry around the Mn^{III} center can be described as a distorted octahedron. As expected for octahedral Mn^{III} complexes, the Jahn−Teller distortion leads to elongated axial bond lengths, in particular for complexes **1**−**4**. The ORTEP drawings of complexes **1**−**5** are shown in Figure 1, and the corresponding molecular arrangements in the crystal lattices are displayed in Figure 2. In the crystal packing of complexes **1**−**5**, two symmetrical arrangements of Mn^{III} dimers are found, the Jahn−Teller distortions of which are also displayed in Figure 2. Their selected bond lengths and angles are summarized in Table 2, while Table 3 lists the "key " bond lengths and angles of complexes **1**−**5** for the discussion of the correlation between the structural features and the Mn^{III}−Mn^{III} magnetic interactions.

Complex 1 with Acetate as the Outer Axial ligand. The Mn^{III} center is coordinated by two nitrogen (N(1) and N(2)) atoms, two phenolate oxygen atoms from saltmen^{2-} (O(1) and O(2)), and two apical oxygen atoms from acetate (O(3)) and the phenolate group (O(2A)) of saltmen^{2-} of the

Table 2. Selected Bond Lengths (Å) and Angles (deg) of Complexes **1**−**5**

1		**2**		**3**	
Mn(1)−O(1)	1.8675(14)	Mn(1)−O(1)	1.879(4)	Mn(1)−O(1)	1.8667(15)
Mn(1)−O(2)	1.8906(13)	Mn(1)−O(2)	1.863(4)	Mn(1)−O(2)	1.8983(14)
Mn(1)−N(1)	1.9778(14)	Mn(1)−N(1)	1.991(4)	Mn(1)−N(1)	1.9677(17)
Mn(1)−N(2)	1.9871(15)	Mn(1)N(2)	1.998(5)	Mn(1)−N(2)	1.9877(17)
Mn(1)−O(3)	2.1130(14)	Mn(1)−N(3)	2.103(6)	Mn(1)−N(3)	2.105(2)
O(1)−Mn(1)−O(2)	91.61(6)	O(2)−Mn(1)−O(1)	90.31(16)	O(1)−Mn(1)−O(2)	93.91(6)
O(1)−Mn(1)−N(1)	93.11(6)	O(2)−Mn(1)−N(1)	166.00(19)	O(1)−Mn(1)−N(1)	91.59(7)
O(2)−Mn(1)−N(1)	164.83(6)	O(1)−Mn(1)−N(1)	93.20(17)	O(2)−Mn(1)−N(1)	163.59(7)
O(1)−Mn(1)−N(2)	170.36(6)	O(2)−Mn(1)−N(2)	91.88(17)	O(1)−Mn(1)−N(2)	167.24(7)
O(2)−Mn(1)−N(2)	91.77(6)	O(1)−Mn(1)−N(2)	163.00(19)	O(2)−Mn(1)−N(2)	89.29(7)
N(1)−Mn(1)−N(2)	81.43(6)	N(1)−Mn(1)−N(2)	80.91(18)	N(1)−Mn(1)−N(2)	82.16(8)
O(1)−Mn(1)−O(3)	97.24(6)	O(2)−Mn(1)−N(3)	95.8(2)	O(1)−Mn(1)−N(3)	97.69(7)
O(2)−Mn(1)−O(3)	95.32(6)	O(1)−Mn(1)−N(3)	98.06(19)	O(2)−Mn(1)−N(3)	100.54(7)
N(1)−Mn(1)−O(3)	98.36(6)	N(1)−Mn(1)−N(3)	97.1(2)	N(1)−Mn(1)−N(3)	94.01(7)
N(2)−Mn(1)−O(3)	91.43(6)	N(2)−Mn(1)−N(3)	98.5(2)	N(2)−Mn(1)−N(3)	93.86(7)

4		**5**	
Mn(1)−O(1)	1.875(7)	Mn(1)−O(1)	1.908(3)
Mn(1)−O(2)	1.918(7)	Mn(1)−O(2)	1.857(3)
Mn(1)−N(1)	1.995(8)	Mn(1)−N(1)	1.979(4)
Mn(1)−N(2)	2.000(9)	Mn(1)−N(2)	1.981(3)
Mn(1)−O(3)	2.014(8)	Mn(1)−O(3)	2.222(3)
O(1)−Mn(1)−O(2)	94.9(3)	O(2)−Mn(1)−O(1)	95.99(12)
O(1)−Mn(1)−N(1)	90.9(3)	O(2)−Mn(1)−N(1)	173.95(13)
O(2)−Mn(1)−N(1)	165.9(4)	O(1)−Mn(1)−N(1)	89.58(13)
O(1)−Mn(1)−N(2)	165.2(3)	O(2)−Mn(1)−N(2)	92.01(13)
O(2)−Mn(1)−N(2)	89.2(3)	O(1)−Mn(1)−N(2)	169.11(13)
N(1)−Mn(1)−N(2)	82.1(3)	N(1)−Mn(1)−N(2)	82.17(14)
O(1)−Mn(1)−O(3)	98.7(3)	O(2)−Mn(1)−O(3)	91.42(13)
O(2)−Mn(1)−O(3)	97.1(3)	O(1)−Mn(1)−O(3)	92.00(12)
N(1)−Mn(1)−O(3)	94.7(3)	N(1)−Mn(1)−O(3)	90.74(14)
N(2)−Mn(1)−O(3)	94.8(4)	N(2)−Mn(1)−O(3)	95.19(14)

Table 3. Pertinent Bond Distances (Å) and Angles (deg) for the Dimeric Cores and Magnetic Parameters of Complexes **1**−**5**, $[Mn(L)(H_2O)]_2(ClO_4)_2$, $[Mn_2(5\text{-Brsalen})(H_2O)_2]_2(ClO_4)_2$, and $[Mn(salen)(H_2O)]_2(ClO_4)_2H_2O$.

	Mn−O	Mn−O*	O−Mn−O*	Mn···Mn* (intradimer)	Mn···Mn* (interdimer)		*g*	D (cm^{-1})	*J* (cm^{-1})	ref
1	1.8906(13)	2.813(5)	99.57(5)	3.641(5)	8.666(1)	F	1.98	−1.9	1.35	this work
2	1.863(4)	3.190(2)	98.39(16)	3.922(5)	8.051(2)	F	1.98	−1.0	0.6	this work
3	1.8983(14)	2.793(0)	97.82(0)	3.584(1)	7.522(1)	F	2.03	−0.3	0.73	this work
4	1.918(7)	2.728(2)	100.00(1)	3.597(3)	9.336(4)	F	2.00	−4.1	0.55	this work
5	1.908(3)	2.395(3)	99.85(11)	3.307(4)	8.920(1)	AF	1.96	−1.0	−0.45	this work
a	1.906(6)	2.419(7)		3.350(3)		AF				24
b	1.912(3)	2.305(2)	76.6(1)	3.181(1)		AF				25
c	1.891(3)	2.490(3)	80.7(1)	3.361(2)		AF				27

[a] $[Mn(L)(H_2O)]_2(ClO_4)_2$ (L = *N*-(acetylacetonylidene)-*N*′-(α-methylsalicylidene)-ethylenediamine). [b] $[Mn_2(5\text{-Brsalen})(H_2O)_2]_2(ClO_4)_2$. [c] $[Mn(salen)(H_2O)]_2(ClO_4)_2H_2O$.

neighboring [Mn(L)(X)] unit. Among them, O(1), N(1), N(2), and O(2) define the basal plane, from which Mn(1) (Mn(1A)) deviates by 0.189 Å. As expected for octahedral Mn^{III} ions, the Jahn−Teller distortion leads to elongated axial bond lengths of Mn(1)−O(3) and Mn(1)−O(2A) (2.1130(14) and 2.813(5) Å, respectively) Within the dimer, the two Mn^{III} ions are linked through the phenolate oxygen atoms (O(1) and O(1A)); the angle of Mn(1)−O(2A)−Mn(1A) is 99.6°, and the two Mn^{III} ions are separated by 3.641(5) Å, which is slightly longer than that of $[Mn_2(saltmen)_2(ReO_4)_2]$[19] and similar to that of $[Mn(3\text{-MeO-salmen})Cl]_2$.[22]

The crystal lattice also contains molecules of acetic acid in addition to the Mn^{III} dimers. There are short interatomic contacts among the atoms of acetic acid and those of the acetate (apical) and the Schiff base ligands: O(4)···H(6B) = 1.772 Å, O(5)···H(19A) = 2.523 Å, O(5)···H(20A) = 2.507 Å, and O(6)···H(22A) = 2.534 Å, as shown in Figure 2a. The shortest interdimer distance of Mn···Mn is 8.666(1) Å, indicating that the magnetic interaction between dimers may be very weak.

Complex 2 with Azido as the Outer Ligand. The basal plane of the Mn^{III} center of complex **2** is again composed of O(1), N(1), N(2), and O(2) from $saltmen^{2-}$. Mn(1) (Mn(1A)) lies above the basal plane by 0.247 Å. The apical positions are occupied by one nitrogen atom of N_3^- with a Mn(1)−N(3) bond length of 2.103(6) Å and the oxygen atom from phenolate group (O(2A)) of $saltmen^{2-}$ of the neighboring [Mn(L)(X)] unit. The bond length of Mn(1)−O(2A) is 3.190(2) Å, which is longer than that of the corresponding bond in complex **1** (2.813 (5) Å). The two Mn^{III} centers within one dimer are connected through the oxygen atoms from phenolate group with a Mn(1)−O(2)−Mn(1A) angle of 98.4°, and they are separated by 3.922(5) Å, which is about 0.3 Å longer than that of complex **1**.

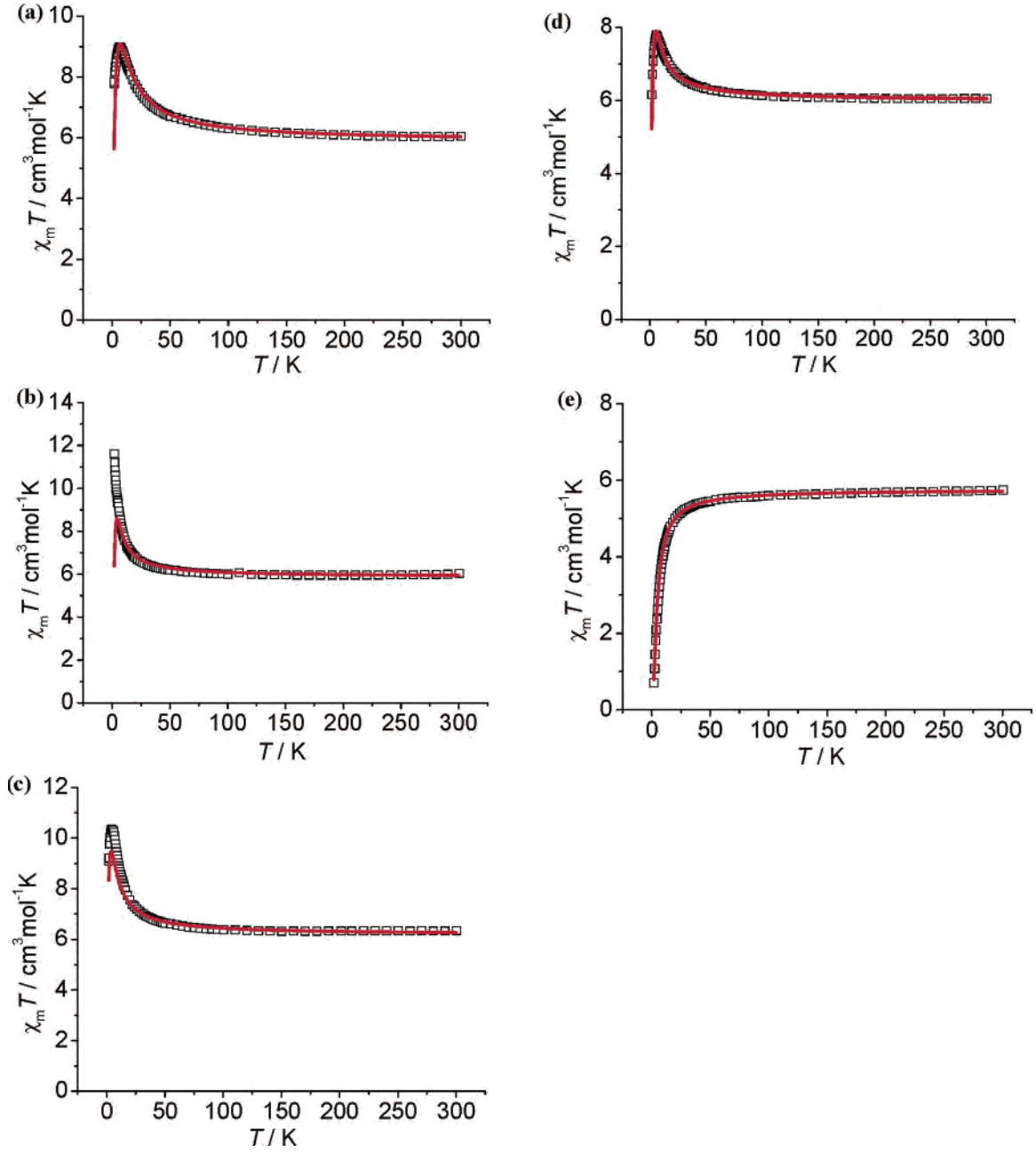

Figure 3. $\chi_m T$ vs T plots for complexes **1**−**5**; the red lines represent a best simulation using an $S_{Mn} = 2$ dimer model described in the text: (a) **1**, (b) **2**, (c) **3**, (d) **4**, and (e) **5**.

The Mn^{III} dimers in the crystal lattice are connected through short interatomic contacts (N(5)···H(20A) = 2.607 Å, N(5)···H(13A) = 2.602 Å) among the nitrogen atoms of the N_3^- apical ligand and the hydrogen atoms of the Schiff base ligand to generate a 2D layer framework (Figure 2b). The Jahn−Teller axes of the Mn^{III} dimers lie in the *bc* plane. The nearest Mn···Mn separation between the dimers is 8.051(2) Å.

Complex 3 with Cyanate as the Outer Ligand. The basal plane of the Mn^{III} center of complex **3** comprises O(1), N(1), N(2), and O(2) from salen^{2-}. Mn(1) (Mn(1A)) lies above the basal plane by 0.223 Å. The apical positions are occupied by one nitrogen atom of NCO^- with the Mn(1)−N(3) bond length of 2.105(2) Å, and the oxygen atom from phenolate group (O(2A)) of salen^{2-} of the neighboring [Mn(L)(X)] unit. The bond length of Mn(1)−O(2A) is 2.793(0) Å, which is shorter than that of the corresponding bond in complexes **1** and **2**. The distance between the two Mn^{III} centers within one dimer is 3.584(1) Å, which is comparable to that of complex **1** and about 0.3 Å shorter than that of complex **2**. Two symmetrical arrangements of Mn^{III} dimers are found in the crystal lattice, and the Jahn−Teller distortions of these two units lie in the *ab* plane, as shown in Figure 2c. No short interatomic contacts are observed among the Mn^{III} dimers, and the nearest Mn···Mn separation between the dimers is 7.522(1) Å, which is slightly shorter than those of complexes **1** and **2**.

Complex 4 with the 3,5-Brsalicyladehyde Anion as the Outer Ligand. The basal plane of Mn^{III} center of complex **4** is composed of O(1), N(1), N(2), and O(2) from 3,5-

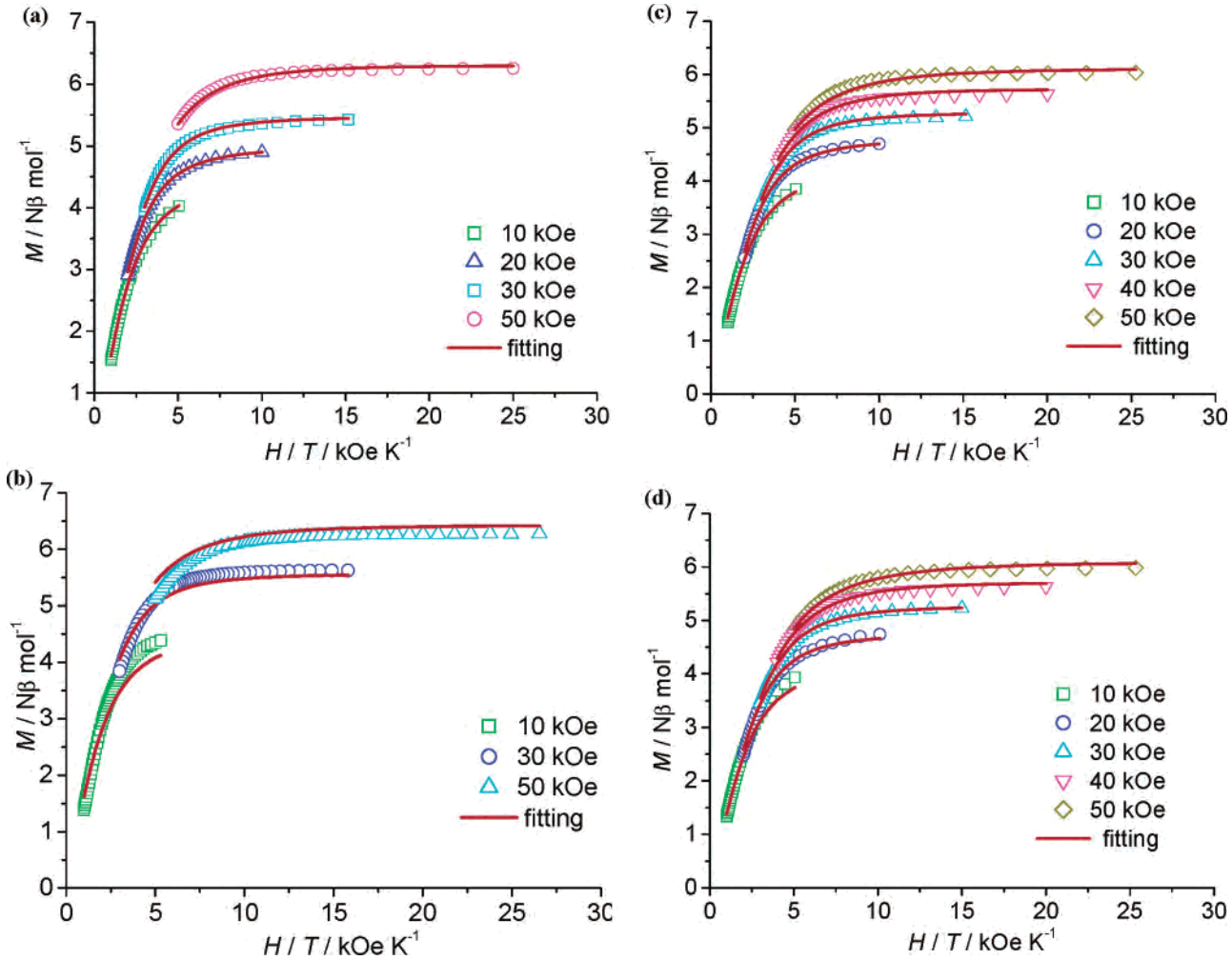

Figure 4. Plots of the magnetization, *M*, vs the ratio of the external field, *H*, to temperature ($T = 2-10$ K) for complexes **1**−**5**; the red lines represent the best fit of the data: (a) **1**, (b) **2**, (c) **3**, and (d) **4**.

Brsalen^{2-}. Mn(1) (Mn(1A)) lies below the basal plane by 0.218 Å. The apical positions are occupied by one oxygen atom of the 3,5-Brsalicyladehyde anion, generated from the decomposition of 3,5-Brsalen, with an Mn(1)−O(3) bond length of 2.014(8) Å and the oxygen atom from phenolate group (O(2A)) of 3,5-Brsalen^{2-} of the neighboring [Mn(L)-(X)] unit. The bond length of Mn(1)−O(2A) is 2.728(2) Å. Again, the two Mn^{III} ions within one dimer are linked by the oxygen atoms from phenolate group, and the angle of Mn(1)−O(2)−Mn(1A) is 100°. The two Mn^{III} ions of one dimer are separated by 3.597(3) Å, comparable to that of complex **3**.

As shown in Figure 2d, there are short interatomic contacts (2.46−2.97 Å) between the bromine and oxygen atoms of the 3,5-Brsalicyladehyde anion (apical ligand) and the hydrogen atoms of the Schiff base ligand. The nearest Mn···Mn separation between the dimers is 9.366(4) Å, obviously longer than those of complexes **1**−**3**.

Complex 5 with Methanol as the Outer Ligand. The basal plane of the Mn^{III} center of complex **5** consists of O(1), N(1), N(2), and O(2) from 5-Brsalen^{2-}. In comparison with complexes **1**−**4**, the Mn^{III} ions are almost lie on the basal planes, and the apical positions are occupied by one oxygen atom of neutral methanol molecule with an Mn(1)−O(3) bond length of 2.222(3) Å and the oxygen atom from phenolate group (O(2A)) of 5-Brsalen^{2-} of the neighboring [Mn(L)(X)] unit, leading to [Mn(L)(X)]$^{+}$. The bond length of Mn(1)−O(2A) is 2.395(3) Å, which is much shorter than those of the corresponding bonds in complexes **1**−**4**. The distance between the two Mn^{III} centers, which are connected by the oxygen atom from the phenolate group with a Mn-(1)−O(2)−Mn(1A) angle of 99.8°, is 3.307(4) Å within one dimer, which is about 0.3 Å shorter than that of complex **1**. In addition to the Mn^{III} dimer, complex **5** contains a perchlorate ion as counterion, the oxygen atoms of which show short contacts (2.50−2.95 Å) with the hydrogen atoms of the Schiff base ligand, as shown in Figure 2e. The nearest Mn···Mn separation between the dimers is 8.920(1) Å.

Magnetic Properties of Complexes 1−5. The temperature dependence of dc magnetic susceptibility of complexes **1**−**5** was measured on polycrystalline samples in the temperature range of 1.9−300 K, as shown in Figure 3. $\chi_m T$ values for these complexes at room temperature are in the range of 5.80−6.23 cm^3 mol^{-1} K (per Mn$^{III}_2$ unit), in good agreement with the 6.0 cm^3 mol^{-1} K value of two noninteracting high-spin Mn^{III} ions ($S = 2$). For complexes **1**−**4**, the $\chi_m T$ value increases gradually upon lowering of the temperature to reach a maximum, indicating a typical ferromagnetic coupling

between Mn^{III} ions. When the temperature is lowered further, a sudden decrease of the $\chi_m T$ value occurs for complexes **1**, **3**, and **4**, which could be mainly regarded as contribution of the zero-field-splitting (ZFS) from Mn^{III} ion. But, the contribution of weak antiferromagnetic interactions between dimers cannot be ruled out. In contrast, for complex **5**, the $\chi_m T$ value keeps decreasing while the temperature decreases from 300 to 1.9 K, in agreement with an antiferromagnetic interaction between Mn^{III} ions. The field dependence of magnetization of complexes **1**−**4** (Figure S1a) supports an overall ferromagnetic interaction for each of them, and the data for complex **5** (Figure S1b) suggest an antiferromagnetic interaction in **5**, since for compounds **1**−**4**, the *M* value quickly increases with the increasing *H* value to above 4.0 Nβ mol^{-1} at 10 kOe, while the *M* value of compound **5** only gets to below 1.0 Nβ mol^{-1} at 10 kOe. The intradimer antiferromagnetic coupling observed for **5** probably originated from the relatively shorter Mn−O* distance in **5** than those of complex **1**−**4**.

The Hamiltonian given in eq 1 has been used to model the magnetic susceptibility ($S_1 = S_2 = S_{Mn}$, S_{iz} is the *z* component of the S_i operator)

$$H = -2JS_1S_2 + D_{Mn}\sum_{i=1,2} S_{iz}^2 + g\mu_B H\sum_{i=1,2} S_i^2 \qquad (1)$$

where *J* is the magnetic coupling constant between two Mn^{III} ions, D_{Mn} is the uniaxial anisotropy of each Mn^{III} ion, *g* is the *g* factor of the Mn ion. The dc susceptibility was simulated using the general procedure developed by Clemente-Juan and co-workers (MAGPACK program) (the solid lines in Figure 3).[33] Because of the long interdimer separations of Mn···Mn (7.522−9.336 Å) in complexes **1**−**5**, the interdimer magnetic interactions may be very weak in terms of the structural view here, so we neglected the influence of interdimer magnetic coupling in fitting the data.[19] The best set of parameters of *g*, *J*, and D_{Mn} are given in Table 3. From these parameters, we can see that the ZFS term, D_{Mn}, is estimated to be in the negative range from −0.3 to −1.9 cm^{-1}, which is consistent with the typical value of −0.38 to −2.53 cm^{-1} for those Mn2 dimer analogues,[22b,23] except for the relatively higher value of −4.1 cm^{-1} for compound **4** for an unknown reason. It is also found that the intradimer interaction parameters, *J*, for complexes **1**−**4** are in the positive range of 0.55−1.35 cm^{-1}, confirming ferromagnetic interaction between Mn^{III} ions, and the values are close to those of reported ferromagnetic Mn^{III} dimers,[23] while the negative *J* value for complex **5** corresponds to an antiferromagnetic interaction between Mn^{III} ions.

Similar to the SMM behavior of $[Mn_2(saltmen)_2(ReO_4)_2]$,[19] the ground state $S_T = 4$ was considered to fit well with the plots of *M* versus *H*/*T* by the least-squares for compounds **1**−**4** (Figure 4). The best-fit D_{Mn2} values for **1**−**4** are −1.03, −0.99, −0.30, and −0.80 cm^{-1}, respectively (solid lines in Figure 4 and Table S1), leading to a theoretical energy barrier, Δ/k_B, of 6.9−23.7 K ($\Delta/k_B = |D_{Mn2}|S_T^2/k_B$, where

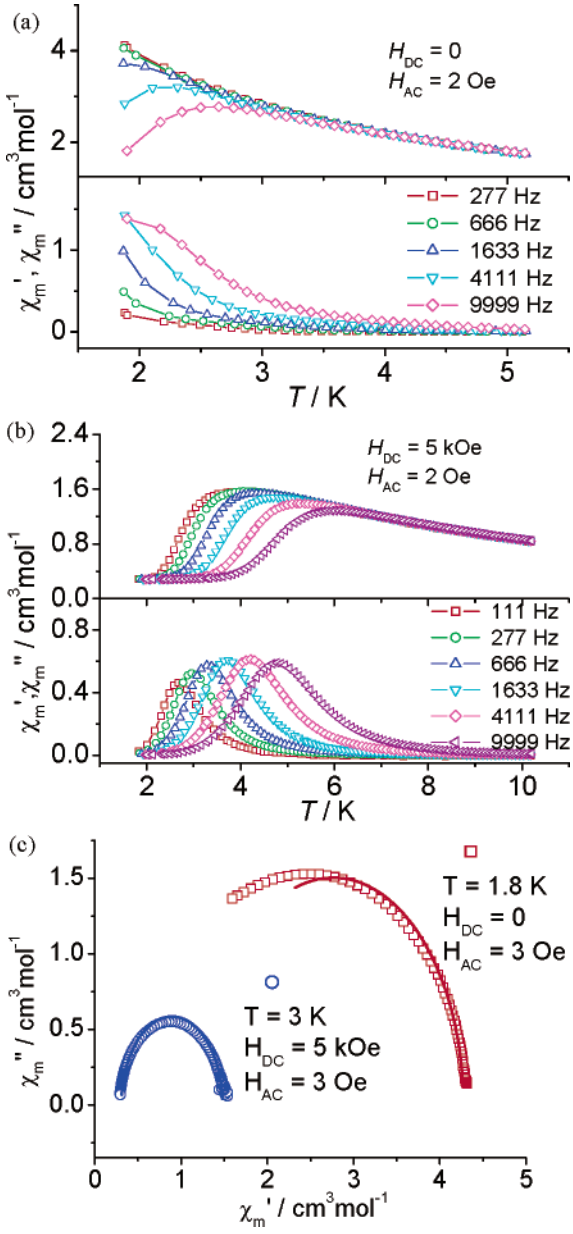

Figure 5. Plots of in-phase (χ_m', top) and out-of-phase (χ_m'', bottom) ac magnetic susceptibility versus temperature (*T*) for complex **1**: (a) under a zero dc field and (b) under a dc field of 5 kOe. (c) The Cole−Cole plot for complex **1**; the solid lines represent the best fit of the data.

k_B is the Boltzmann constant). The Δ/k_B value of compound **3** is the smallest because of its relatively low D_{Mn2} value.

The measurement of the ac magnetic susceptibility at low temperature was performed on polycrystalline samples of complexes **1**−**4** (Figures 5−8). The plots under zero-applied dc field all show frequency dependence, as expected for SMMs, although they do not show maxima peaks, except for compound **2**. When the dc field is increased to 5 kOe for compound **1** and 1 kOe for compounds **2**−**4**, the in-phase and out-of-phase maxima peaks both shifted to the direction of higher temperature and could be easily observed above 2 K. This may be caused by the coexistence of the thermal and tunneling processes for magnetic relaxation. The tunneling process shortened the magnetic relaxation time at a zero dc field. According to the Arrhenius equation ($\tau = \tau_0 \exp(E_a/k_BT)$, $\tau = 1/(2\pi f)$, and *T* is the temperature at which

(33) Borrás-Almenar, J. J.; Clemente-Juan, J. M.; Coronado, E.; Tsukerblat, B. S. *J. Comput. Chem.* **2001**, *22*, 985.

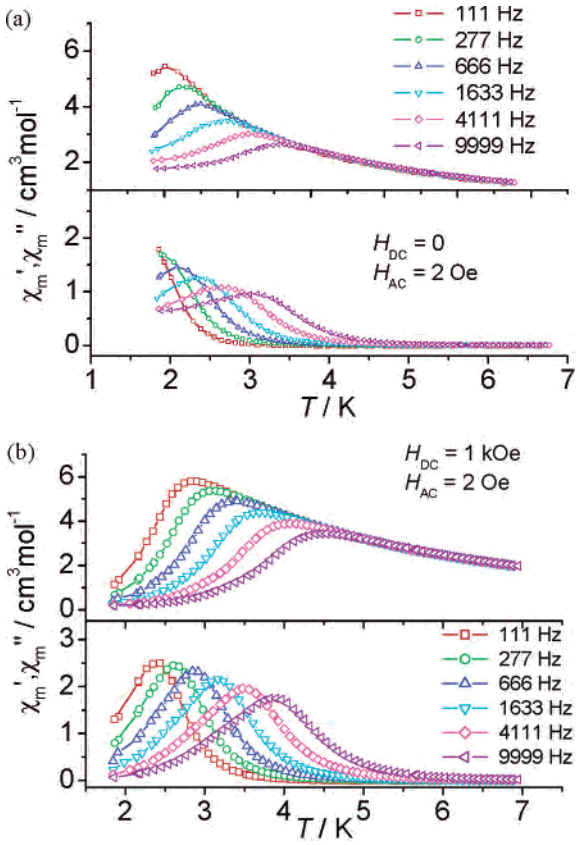

Figure 6. Plots of in-phase (χ_m', top) and out-of-phase (χ_m'', bottom) ac magnetic susceptibility versus temperature (T) for complex **2**: (a) under a zero dc field and (b) under a dc field of 1 kOe.

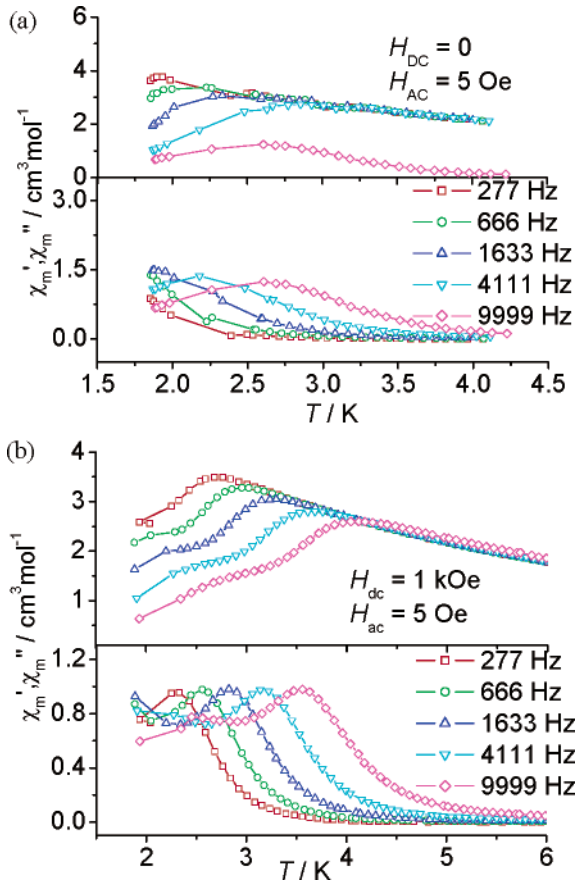

Figure 7. Plots of in-phase (χ_m', top) and out-of-phase (χ_m'', bottom) ac magnetic susceptibility versus temperature (T) for complex **3**: (a) under a zero dc field and (b) under a dc field of 1 kOe.

the maximum of the χ_m'' occurred under different f (frequency) values from 111 to 9999 Hz), activation energy E_a/k_B, and a pre-exponential factor, τ_0, were deduced (Figure S3). Note that we applied a static dc field to avoid tunneling at a zero-applied field. On the other hand, the quantum tunneling of the magnetization at a zero field can reduce the energy barrier, E_a/k_B, as seen in other SMM systems.[19,34] In agreement with this idea, the value of E_a/k_B should be increased with an increase of the applied dc field. To take compound **2** as an example, from its curve of χ_m'' versus T under a zero dc field, an activation energy, E_a/k_B, of 17 K was deduced following the Arrhenius law. This value of E_a/k_B is lower than the expected value calculated from D_{Mn2} ($\Delta/k_B = |D_{Mn2}|S_T^2/k_B = 23$ K). When a *dc* field of 1 kOe was applied, the E_a/k_B value increased to 29 K (Figure S3b).

At a fixed temperature and a zero dc field or a certain applied field, the χ_m' and χ_m'' values were also measured as a function of the ac frequency, f, ranging from 10 to 10 000 Hz. From these measurements, Cole−Cole diagrams (χ_m'' vs χ_m' plots) have been obtained for complexes **1**−**3** (Figure 5c and Figure S2) and have been simulated using a generalized Debye model (the solid lines).[35] The representative Cole−Cole plots are depicted in Figure 5c for complex **1**. The best-fit parameters for the χ_m'' versus χ_m' plot at 1.8 K under a zero dc field are $\chi_s = 1.26$ cm^3 mol^{-1}, $\chi_T = 4.28$ cm^3 mol^{-1}, $\tau = 4.2 \times 10^{-5}$ s, and $\alpha = 0.10$; the best-fit results for the χ_m'' versus χ_m' plot at 3.0 K under a 5 kOe dc field are $\chi_s = 0.31$ cm^3 mol^{-1}, $\chi_T = 1.48$ cm^{-1} mol^{-1}, $\tau = 3.7 \times 10^{-4}$ s, and $\alpha = 0.10$, where χ_s is the adiabatic susceptibility, χ_T is the isothermal susceptibility, τ is the average relaxation time of magnetization, and the α parameter ranges between 0 and 1, quantifying the width of the τ distribution. As for those fitting parameters, the α parameters are very similar, whereas the values of χ_s, χ_T, and τ have obvious differences. The applied dc field of 5 kOe increased the resulting relaxation time (τ) in contrast with the value under a zero dc field, in agreement with the conclusion reached from the χ_m'' and χ_m' versus T plots at different frequencies.

Strangely, the ac susceptibility of compound **3** measured under a 1 kOe dc field shows another weak magnetic relaxation course at lower temperature, shown by the frequency dependence, in addition to the one at higher temperature (Figure 7). The Cole−Cole circles measured on an applied dc field of 1 kOe at temperatures of 1.8−3.5 K clearly display two semicircles at 1.8 K confirming the

(34) Costes, J. P.; Dahan, F.; Wernsdorfer, W. *Inorg. Chem.* **2006**, *45*, 5.

(35) (a) Cole, K. S.; Cole, R. H. *J. Chem. Phys.* **1941**, *9*, 341. (b) Boettcher, C. J. F. *Theory of Electronic Polarization*; Elsevier: Amsterdam, 1952. (c) Aubin, S. M.; Sun, Z.; Pardi, L.; Krzysteck, J.; Folting, K.; Brunel, L. J.; Rheingold, A. L.; Christou, G.; Hendrickson, D. N. *Inorg. Chem.* **1999**, *38*, 5329. (d) Miyasaka, H.; Clérac, Mizushima, K.; Sugiura, K.; Yamashita, M.; Wernsdorfer, W.; Coulon, C. *Inorg. Chem.* **2003**, *42*, 8203.

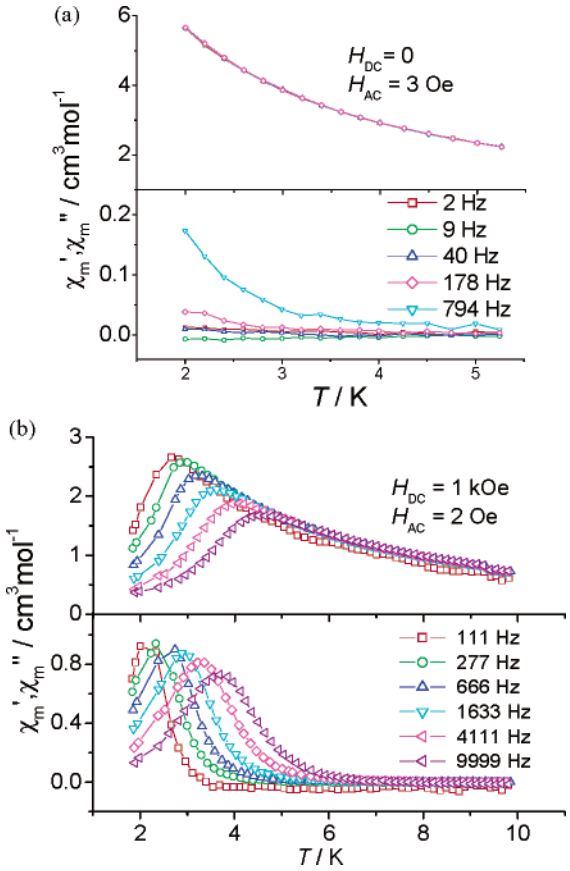

Figure 8. Plots of in-phase (χ_m', top) and out-of-phase (χ_m'', bottom) ac magnetic susceptibility versus temperature (T) for complex **4**: (a) under a zero dc field and (b) under a dc field of 1 kOe.

presence of two magnetic relaxation courses below 1.8 K. When the temperature was increased to 2.5 K, one of the two magnetic relaxation courses begins to degenerate, and it completely disappeared at 3.0 K. This phenomenon may be caused by the weak intermolecular interaction since the nearest interdimer Mn−Mn distance is 7.522(1) Å, relatively shorter than those of compounds **1**−**3**.[36]

Discussion on Correlation between Structure and Magnetic Behavior. According to Table 3, the Mn^{III}−O* distances of the ferromagnetic interacting dimers, **1**−**4**, were found to be relatively longer than that of **5** and the other reported complexes, within which the two Mn^{III} ions interact antiferromagntically.[23−25,27] On the basis of the bond lengths and angles, in particular the unequal bond lengths of two apical bonds observed for complexes **1**−**4** as described above (see Table 3), Jahn−Teller distortion occurs at each Mn^{III} center. However, as a whole the coordination geometry around each Mn^{III} center is close to being an octahedron. Thus the ferromagnetic interaction between Mn^{III} ions for complexes **1**−**4** could mainly be the result of the d_{z2} and d_π orbitals (d_{xy}, d_{yz}, and d_{xz} orbitals) orthogonality.[23] The antiferromagnetic interaction due to the Mn^{III}−O* bonds with comparably long bond lengths may be rather weak. For complex **5**, however, the Mn^{III}−O* bond length is relatively short (2.395(3) Å), and the observed antiferromagnetic interaction between Mn^{III} ions is probably the result of the antiferromagnetic interaction due to the Mn^{III}−O* bonds becoming dominant. The correlation between the Mn^{III}−O* distances and the magnetic exchange parameters, J_F (1.35 cm^{-1} for **1** and 0.6 cm^{-1} for **2**), for compounds **1** and **2** can follow with the equation[23]

$$J_F = 4.5724 - 1.1868x \qquad (2)$$

where x = Mn···O* distance (Å) in the range of 2.4−3.7 Å and the calculated J_F values are 1.23 and 0.79 cm^{-1} for complexes **1** and **2**, respectively (see Figure S4). In all, it can be concluded that ferromagnetic Mn^{III} dimers may show SMM behavior, while the Mn^{III}−O* distances may be the main factor determining if the magnetic coupling is ferromagnetic or antiferromagnetic. Also, it is noteworthy that the anisotropy of a Mn^{III} ion (ZFS term) depends significantly on the Jahn−Teller distortion that leads to a negative ZFS parameter in our Mn_2 dimer compounds, **1**−**4**.[37]

Summary

The syntheses, crystal structural characterization, and magnetic properties of five new Mn^{III} dimers bridged by phenolate oxygen atoms were described. Complexes **1**−**4** exhibit intradimer ferromagnetic exchange and display frequency dependence of ac magnetic susceptibility, probably showing the characteristic SMM behavior. These results will enrich the SMM studies. In contrast, complex **5** shows an intradimer antiferromagnetic coupling probably originating from the relatively shorter Mn−O* distance. Although it is still difficult to find a clear correlation between the Mn···Mn magnetic interaction and the structural features of these Mn^{III} dimeric complexes, it may be concluded that the Mn···Mn magnetic interaction can be modulated by varying the tetradentate Schiff base and apical ligands. Moreover, these new Mn^{III} dimer complexes could be used as building blocks to obtain versatile polymeric architectures by introducing other magnetic subunits as suggested by Miyasaka et al.[38]

Acknowledgment. The present research was financially supported by NSFC (20421101, 20372066, 20490210, and 20221101), Chinese Academy of Sciences, and State Key Basic Research Program. D.-Q.Z. and S.G thank the National Science Fund for Distinguished Young Scholars. The authors also thank the anonymous reviewers for their suggestions and comments which allowed us to largely improve the manuscript.

Supporting Information Available: CIF files of the crystal structures of complexes **1**−**5**, M versus H plots for complexes **1**−**5**, Cole−Cole diagrams for complexes **2** and **3,** Arrhenius plots of ln τ versus $1/T$ for complexes **1**−**4**, and the plot of the correlation between the ferromagnetic exchange parameters, J, and the Mn−O* distances for **1** and **2** and related compounds. This material is available free of charge via the Internet at http://pubs.acs.org.

IC051648L

(36) Boskovic, C.; Bircher, R.; Tregenna-Piggott, P. L. W.; U. Güdel, H.; Paulsen, C.; Wernsdorfer, W.; Barra, A. L.; Khatsko, E.; Neels, A.; Stoeckli-Evans, H. *J. Am. Chem. Soc.* **2003**, *125*, 14046.

(37) Gerritsen, H. J.; Sabinsky, E. S. *Phys. Rev.* **1963**, *132*, 1507.

(38) (a) Miyasaka, H.; Matsumoto, N.; Okawa, H.; Re, N.; Gallo, E.; Floriani, C. *J. Am. Chem. Soc.* **1996**, *118*, 981. (b) Miyasaka, H.; Clérac, R. *Bull. Chem. Soc. Jpn.* **2005**, *78*, 1725.